Egyptian Journal of Chemistry
http://ejchem.journals.ekb.eg/

GC–MS and Molecular Docking Analyses of Phytochemicals from *Calendula officinalis* L. Hexane Extract and Evaluation of its Antioxidant and Wound Healing Properties in Rats

Abeer Salama[a], Mahitab I. EL-Kassaby[b*], Ahmed Refaat[c,d], Rasha M.M. Mohasib[e]

[a]*Pharmacology Department, National Research Centre, El-Buhouth St, Dokki, Cairo 12622, Egypt*
[b]*Medical Physiology Department, National Research Centre, El-Buhouth St, Dokki, Cairo 12622, Egypt*
[c]*Spectroscopy Department, National Research Centre, 33 El-Bohouth St., 12622, Dokki, Giza, Egypt.*
[d]*Molecular Modeling and Spectroscopy Laboratory, Centre of Excellence for Advanced Science, National Research Centre, 33 El-Bohouth St., 12622, Dokki, Giza, Egypt.*
[e]*Plant Biochemistry Department, National Research Centre, 33 El-Bohouth St., 12622, Dokki, Giza, Egypt.*

Abstract

Wound healing stays a substantial health affair for a great number of patients globally. Hypoxia plays a decisive role in specifying the normal successfulness of healing process. Hypoxia-inducible factor-1alpha, plays a critical role in oxygen homeostasis, cell survival and migration and growth factor release throughout the healing process. The target of this research is to characterize the phytochemical and antioxidant analysis of the lipophilic extract of *Calendula officinalis* (*C. officinalis*) flowers utilizing colorimetric, spectrophotometric, and chromatographic techniques. In addition, studying the wound healing properties *in vivo* and *in vitro* model. Rats were divided into four groups (six in each group) as follow: Group I: Control rats. Group II: Wounded and untreated rats. Group III: Rats are treated topically with 2.5% of *C. officinalis* in gel. Group IV Rats are treated topically with 5% of *C. officinalis* in gel. Furthermore, Molecular docking study was conducted to elucidate the mechanistic of *C. officinalis* wound healing properties through the inhibitory effects of its main components against key antihealing goals and study the best binding affinity. Using GC-MS analysis seven main different organic classes fatty acid (19.45%), fatty alcohol (17.54%), sesquiterpene (34.9%), hydrocarbons (20.06%), diterpene (3.9%), phytosterol (2.10%) and alkaloid (0.53%), and 24 components comprising 98.48% of the observed peaks were identified as a consequence. Clearly, 1-heptatriacotanol (16.47%) is the most abundant fatty alcohol. Additionally, Isochiapin B is a significant sesquiterpene compounds that accounting for 15.91% of all sesquiterpene compounds. Moreover, this extract exhibited potent antioxidant activity as demonstrated by the IC_{50}. Owing to its high concentration of active compounds, *C. officinalis* promoted wound contraction, collagen synthesis, 5' adenosine monophosphate-activated protein kinase (AMPK) elevation, Hypoxiainducible factor 1-alpha (HIF-1α) elevation and accelerated epithelization with a decrease in matrix metalloproteinases (MMP-9). Molecular docking revealed that Isochiapin B had better binding affinities than 1-Heptatriacotanol in the interaction with AMPK, Collagenase, HIF-1α, MMP-9, tumor necrosis factor alpha (TNF-α), and vascular endothelial growth factor (VEGF), and its best binding affinity was with MMP-9. Obtained results assured that *C. officinalis* L possesses considerable wound healing activity in wounded rats due to its potent antioxidant and anti-inflammatory effects.

Keywords: *Calendula officinalis*, Isochiapin B, Wound healing, Hypoxia; AMPK, oxidative stress, antioxidant activity.

1. Introduction

The process of healing a wound is an intricate and multifaceted one that includes four distinct stages, namely hemostasis, inflammation, proliferation, and tissue remodeling [1]. Any of these phases that are disrupted or irregular will cause poor healing. Long-term wounds or ulcers, particularly patients with chronic illnesses including ischemic heart disease, diabetes mellitus and hypertension, have severe and complex situations [2]. A disruption in the cell continuity of the skin's regular anatomical structure can be caused by mechanical damage (such as surgery), thermal conditions (such as burns), or physiological defects (such as diabetes and malignancy) [3]. Wound healing is considered as the toughest medical cases for patients [4]. Wound healing process is intricate and involves several carefully controlled events. An acute wound becomes a chronic wound if this process is delayed. Increased tissue destruction and necrosis rather than healing arise from the cascade of healing process being disrupted in severe pathological situations. This is often linked to oxidative stress and the chronic inflammation.

In the early stages of inflammation, wound sites are frequently hypoxic with a disturbance of the vasculature surrounding the wound, which impairs the delivery of oxygen, and worsen by the sudden influx of inflammatory cells which are essential for granulation and re-epithelialization [5]. Hypoxia dramatically enhances the proliferation of human dermal releasing transforming growth factor-β1 (TGFβ1). Acute hypoxia therefore causes a brief rise in cellular replication and aids in the start of the healing process [6]. In stages of vascular homeostasis, endothelial cells of different sources express AMP activated protein kinase (AMPK) [7]. Activated AMPK supports vascular homeostasis, suppresses

*Corresponding author e-mail: m_mahy10@hotmail.com.; (Mahitab I. EL-Kassaby).
Receive Date: 16 October 2024, Revise Date: 01 November 2024, Accept Date: 11 November 2024
DOI: 10.21608/ejchem.2024.328645.10642

reactive oxygen species (ROS) and defenses against apoptosis. Hence, AMPK activation has been linked to angiogenesis and wound healing [8].

C. officinalis is a native of Mediterranean region. It is a member of the *Asteraceae* family. It spreads widely in a variety of sunny locations with humid atmospheric conditions [9,10]. *C. officinalis* is an annual herb with many different parts, including flowers and leaves. In Old English, calendula is known as "gold." The genus of Calendula contains approximately twenty-five species, *C. officinalis*, C. *stellata, C. arvensis*, *C. tripterocarpa*, and *C. suffruticose* are the most frequent. *C. officinalis* has been utilized since the 12th century for medical purposes [11,12]. Extracts from the flowers of *C. officinalis*, also known as pot marigolds, have a long history in ethnopharmacology [13]. It has been used in the pharmaceutical industry because of different ingredients such as flavonoids, saponins, carotenoids, sterols, phenolic acids, amino acids, carbohydrates, aromatics, vitamins, minerals, etc. [14,15]. These ingredients exhibit anti-inflammatory, antioxidant, antiaging, anti-tumor, gastrointestinal, ulcers diuretic, and for anemic women, splenic and hepatic inflammations, mental tension as well as insomnia-related disorders [16-18]. Other pharmacological properties of *C. officinalis* involve antiviral, antimicrobial,
treatment of breast cancer, and antiimmunomodulatory effect, treatment of acne, wound healing properties, anti-gastric ulcer, anti-bacterial infections in animals, renal protective effect [19]. In addition, Hexane also effectively extracts aroma compounds, such as phenylpropenes, sesquiterpenes, triterpenes, as well as, tocopherols, and saturated and unsaturated fatty acids, which may have antioxidant, anti-aging and useful for the healing of skin wounds; because of their strong anti-inflammatory properties, they additionally help in the healing process by lowering inflammation and creating an environment that is favorable to tissue repair [20-24].

This study is carried out to evaluate uniquely phytochemical constituents in lipophilic extract of *C. officinalis* flowers and highlight its mechanistic perspective in wound healing *in vivo* model and its antioxidant activity by different models *in vitro*. Furthermore, molecular docking investigates the best binding affinity.

2. Material and methods

2.1. Plant material

Relevant institutional, national, and international rules and laws are followed in the collecting of plants and experimental research conducted on the plant used for the study. The study utilized fresh *C. officinalis* (Asteraceae) flowers that were gathered from the Medicinal Plants Station at the Faculty of Pharmacy, Ain Shams University (Cairo) in June 2022. The plant name has been checked with http://www.theplantlist.org (accessed in April 2024). The flowers' authenticity was identified by a plant taxonomist at the Ministry of Agriculture. With voucher numbers (M227), voucher specimens were deposited in the National Research Centre herbarium. The deposit material is accessible to the public herbarium. The plant material was identified and then prepared for extraction.

2.2. Preparation and Extraction of *Calendula officinalis*

Fresh flowers were washed with flowing distilled water, left to air-dry at room temperature, Briefly, dry flowers were powdered by a professional herb's grinder and macerated in distilled n-hexane for seven successive days. After filtration, the extract was evaporated under reduced pressure at 40°C using a rotary-type evaporator (Büchi, Switzerland). Before being used, the resultant crude extracts were collected and stored at -20°C until needed.

2.3. Determination of dry matter content

By rotary evaporator under vacuum at 40°C, the extract was concentrated to obtain crude lipophilic extract. Additionally, the following process was used to calculate, express as a percentage, and determine the extract yield. X extract is extraction yield expressed in % (w/w).

X extract % = [(Weight of dry extract(g)) / (Weight of dry plant(g)) × 100]

Following that, the *C. officinalis* lipophilic extract was kept for later analysis at 4°C.

2.4. Analysis of Phytochemicals

2.4.1. Screening for phytochemicals in a qualitative methodology

Phytochemical screening of hexane extract of *Calendula officinalis* was carried out via standard procedures according to standard methods to determine the presence of steroids, terpenoids, alkaloids, phenols, tannins, flavonoids, saponins, glycosides, reducing sugars, Quinones and coumarins according to standard methods of Harborne [25]. A positive reaction to these tests was characterized as any color change or precipitate development.

2.4.2. Estimation of total phenolic compound content

Using gallic acid as a standard, the total phenolic (TP) of the lipophilic extract was measured using a spectrophotometer and the Folin-Ciocalteu reagent test at 760 nm. Gallic acid solution was used to produce the standard curve, and the amount of gallic acid equivalent in milligrams per gram of plant dry

extract (mg GAE/g extract) was used to compute the TPC [26].

2.4.3. Estimation of total tannin content

Tannic acid was used as a reference to determine the total tannin (TT) of the extracts using a spectrophotometer and Folin-Ciocalteu's reagent at 775 nm. According to Tempel [27] approach, total tannins were quantified as mg of tannic acid equivalent (TAE)/g of dry extract.

2.4.4. Estimation of flavonoid content

The flavonoid content of the extract was ascertained using the aluminum trichloride ($AlCl_3$) test. At 510 nm, the absorbance was measured. The standard curve was created using quercetin as a reference, and the flavonoid content was expressed as milligrams of quercetin equivalent per gram of plant dry extract (mg QE/g DE) [28].

2.4.5. Identification of non-polar compound by gas chromatography/mass spectrometry analysis

The lipophilic extract's chemical constituents were identified using GC-MS analysis. A computer was used to determine the percentage composition of each component based on the entire chromatogram. Using reference samples and a NIST library search, several chemicals were found based on their retention time and peak enhancement [29].

2.5. Evaluation of the antioxidant potential

2.5.1. Free radical scavenging activity (DPPH)

When antiradical substances are present, the free radical 1,1-diphenyl-2-picrylhydrazyl (DPPH), which has a violet color, is diminished. The measurements of absorbance were taken at 517 nm. Butylated hydroxyl toluene was used as positive controls, or standard. As a negative control, DPPH solution was employed. The procedure was carried out in a triplicate manner, then using the following formula, the inhibition percentage is determined [30].

DPPH %= [(Abs control – Abs sample/Abs control) × 100]

The radical scavenging activity (RSA) curve's slope equation is used to determine the IC_{50} value, which is the concentration of the sample that can block 50% of free radicals.

2.5.2 $ABTS^+$ Scavenging Activity

Using the procedure described by Re et al. [31]. ABTS [2,2′-azinobis (3- ethylebenzothiozoline-6sulphonic acid)], a radical cation decolorization assay, was also utilized to examine the lipophilic extract's capacity to scavenge free radicals. In this experiment,

Trolox served as the standard. Using a UV spectrophotometer, the absorbance of each sample was measured for potential inhibition at a wavelength of 734 nm. The calculation of the inhibition percentage (%) formula.

$ABTS^{\cdot+}$ % inhibition = [(Abs control – Abs sample/Abs control) × 100]

The ABTS free radical scavenging activity was reported in terms of IC_{50} (µg/mL).

2.5.3. Hydrogen peroxide scavenging activity (H_2O_2)

Using the procedure described by Re et al. [31]. ABTS [2,2′-azinobis (3- ethylebenzothiozoline-6sulphonic acid)], a radical cation decolorization assay, was also utilized to examine the lipophilic extract's capacity to scavenge free radicals. In this experiment,

Trolox served as the standard. Using a UV spectrophotometer, the absorbance of each sample was measured for potential inhibition at a wavelength of 734 nm. The calculation of the inhibition percentage (%) formula.

$ABTS^{\cdot+}$ % inhibition = [(Abs control – Abs sample/Abs control) × 100]

The ABTS free radical scavenging activity was reported in terms of IC_{50} (µg/mL).

2.5.3. Hydrogen peroxide scavenging activity (H_2O_2)

The method of Ruch et al. [32] was used to determine the lipophilic extract's capacity to scavenge hydrogen peroxide (H_2O_2). The positive control was ascorbic acid. The following formula was used to determine the extracts' capacity to scavenge H_2O_2: At 230 nm, the absorbance was measured. The following formula was used to determine the extracts' capacity to scavenge H_2O_2 and the IC_{50} values were determined.

H_2O_2 scavenging activity (%) = [(Abs control – Abs sample/Abs control) × 100]

2.5.4. Iron chelating assay

Using the method of Dinis et al 1994 [33] the chelating activity on ferrous ions (Fe^{2+}) was measured by extract or EDTA solution as a positive control at varied concentrations. A spectrophotometric measurement of the solution's absorbance at 562 nm was made. Both the IC_{50} and the inhibition % of the formation of the ferrozine Fe^{2+} complex was recorded.

Chelating rate (%) = [(Abs control – Abs sample/Abs control) × 100]

2.6. Animals

Twenty-four Wister albino male rats, weighing between 150 and 170 g each, were taken from the colony section of the National Research Centre (NRC), Egypt. Rats were kept at a controlled temperature and humidity (23± 2°C/45-55% relative humidity). Throughout the trial, they lived in separate, clean cages and were given access to ad libitum tap water and pelleted food.

2.7. Chemicals

Skin contents of collagen, matrix metalloproteinases (MMP9), AMPK and Hypoxia-inducible factor-1 (HIF-1) were evaluated using enzyme-linked immunosorbent assay (ELISA) kits (Sunlong Biotech Co., Ltd, China).

2.8. Experimental protocol

The biological evaluation of the topical application of *C. officinalis* flowers was performed using a fullthickness wound model in rats, where, the rats' dorsal skin was shaved the day before the experiment. The full-thickness skin excision circular wound (5 mm in diameter) was produced under light anesthesia using a sterile biopsy punch needle (No.5, Ribbel International Ltd., India). A flap of skin was removed from each side of the rats' spine, revealing the muscular fascia, as previously reported [34]. Rats were divided into four groups (six in each group) as follow: Group I: Control rats. Group II: Wounded and untreated rats. Group III: Rats are treated topically with 2.5% of *C. officinalis* in gel (2.5 g extract incorporated into 100 g gel base). Group IV Rats are treated topically with 5% of C. officinalis in gel (5 g extract incorporated into 100 g gel base) [35,36].

All treatments were applied topically, daily for ten days. In addition, a normal control group and positive control. Rats sacrificed by cervical dislocation under anesthesia (ketamine, 70 mg/kg, i.p) once more and on the tenth day post-wounding. The wounded tissues were excised and divided into two parts. Part I was homogenized and the supernatant was evaluated for further biochemical indices. Part II was fixed in 10% formol saline.

2.9. Morphology of the wounds

The reduction in wound area was measured at 0, 3, 7 and 10 days after the start of the experiment to evaluate the wound healing. The following equation was used to compute the relative reduction in wound area:

Relative reduction in wound area (%) = $\frac{A_o - A_t}{A_o}$ x 100

Where, A_o and A_t are the wound area at zero time and time (t), respectively. The wound was photographed with the Huawei FLA-LX1 smart phone camera, resolution of 8 megapixels) to be evaluated with ImageJ (http://rsbweb.nih.gov/ij/download.html) [37].

2.10. Biochemical indices

Wounded skin samples from various groups of rats were taken 10 days following wounding. In order to prepare 20% (w/v) homogenates in phosphate buffer (pH 7.4), a homogenizer (Medical Instruments, MPW120, Poland) was employed. To precipitate cell debris, the homogenates were centrifuged for 10 minutes at 1000 rpm and 4°C using a cooling centrifuge (2 k15, Sigma, Germany). Supernatants were collected for evaluating skin content of collagen, MMP9, AMPK and HIF-1α [38].

2.11. Histopathological examination of skin samples

Autopsy samples were taken from the skin of rats in different groups and fixed in 10% formol saline for twenty-four hours. Washing was done in tap water then serial dilutions of alcohol (methyl, ethyl and absolute ethyl) were used for dehydration. Specimens were cleared in xylene and embedded in paraffin at 56 degrees in hot air oven for twenty-four hours. Paraffin bees wax tissue blocks were prepared for sectioning at 4 microns' thickness by rotary LEITZ microtome. The obtained tissue sections were collected on glass slides, deparaffinized, stained by hematoxylin and eosin stain for examination through the light electric microscope [39].

2.12. Statistical analysis

For three replications, the mean ± SD was used to express all in vitro data. The data were statistically analyzed using analysis of variance, and the significance of the results was determined using the Duncan test. This allowed for numerous comparisons of the data to identify the significant differences among them. Differences were deemed significant if $p< 0.05$. The statistical analysis was performed using SPSS version 19.0.

One-way analysis of variance (ANOVA) and Fisher's LSD comparison test were used for all quantitative comparisons in the in vivo investigation (GraphPad Prism 8.0, USA). The data are presented as the mean ± SD of six rats, and a significant difference was identified when the $p< 0.05$.

2.13. Molecular docking

Molecular docking is a very useful approach in studying the interaction between a ligand and a protein by predicting the binding affinity, such that the lowest generated score (in Kcal/mol) represents the best the binding affinity [40]. In the current study, molecular docking was performed to investigate the binding modes between the two compounds 1-heptatriacotanol and isochiapin B, and six proteins AMPK, collagenase, HIF-1α, MMP-9, tumor necrosis factor alpha (TNF-α), and vascular endothelial growth factor (VEGF).

2.13.1 Ligand preparation

The 3D structure of 1-Heptatriacotanol was downloaded from ChemSpider (http://www.chemspider.com/ accessed on 3 February 2024) (ChemSpider CID: 467776), while that of isochiapin B was built in GaussView 5.0 software. The structures were then optimized using GAUSSIAN 09 software [41] at Molecular Modeling and Spectroscopy Laboratory, Centre of Excellence for Advanced Science, National Research Centre, Egypt. Optimization was done by density functional theory (DFT) method using the B3LYP functional [42-44] and the 6-31G (d,p) basis set. The DFT optimized structures were finally saved in pdb format to be submitted for the dockings study.

2.13.2. Protein preparation

The 3D crystal structures of AMPK, collagenase, HIF-1α, MMP-9, TNF-α, and VEGF were retrieved from the Protein Data Bank as PDB ID: 4zhx [45], 1cgl [46], 3kcx [47], 1gkc [48], 2AZ5 [49], and 1flt [50], respectively. Using BIOVIA Discovery Studio Visualizer, the structures were prepared by removing all water molecules then further purified by removing hetatoms and co-crystallized ligands. The cleaned structures were then subjected to energy minimization which was performed in vacuo using GROMOS96 43B1 Force-Field implementation in Swiss PdbViewer software (version 4.1.0) [51]. Docking was then performed using AutoDock 4.2 software (The Scripps Research Institute, La Jolla, San Diego, CA, USA) [52]. First, polar hydrogen atoms were added, nonpolar hydrogen atoms were merged, and Gasteiger charges were applied. All of the docking calculations were performed utilizing Lamarckian genetic algorithm and a total of 100 GA runs for each calculation. All other parameters were kept as default. For docking, to cover the active sites the grid box was generated with the dimensions 50 Å x 55 Å x 60 Å, centered at (79.551, 13.946, 32.678) for AMPK; 60 Å x 60 Å x 60 Å, centered at (30.681, 46.555, -0.009) for collagenase; 60 Å x 73 Å x 50 Å, centered at (-20.648, 30.887, 8.156) for HIF-1α; 45 Å x 42 Å x 57 Å, centered at (64.179, 30.866, 115.866) for MMP-9; 28 Å x 26 Å x 30 Å, centered at (-19.515, 74.840, 33.894) for TNF-α; and 100 Å x 60 Å x 100 Å, centered at (0.742, -0.592, 16.909) for VEGF. The molecular docking results were analyzed in BIOVIA Discovery Studio Visualizer.

3. Results

3.1. Extraction yield

The yield and the percentage mass of lipophilic extract of *C. officinalis* is 14.32g and 14.32%. As well as, we obtained dark orang pigmentations. Additionally, the crude extract was Waxy texture that will appear in the final product (Table1).

3.2. Qualitative phytochemical screening

In the present investigation the qualitative phytochemical analysis of hexane extract of *C. officinalis* is carried out as proved in Table 2. Terpenoids, steroids, phenols, flavonoids, tannins, saponins, alkaloids, Quinones and coumarins were detected in this extract.

3.3. Quantitative phytochemical analysis

C. officinalis flower possessed total phenolic content (TPC), total tannin (TTC) and total flavonoid (TFC) was shown in Figure 1, expressed as gallic acid, tannic acid and quercetin equivalents, were 66.36 ±0.48, 53.57 ±1.10 and 45.06 ±3.85 mg/ /g dry extract respectively.

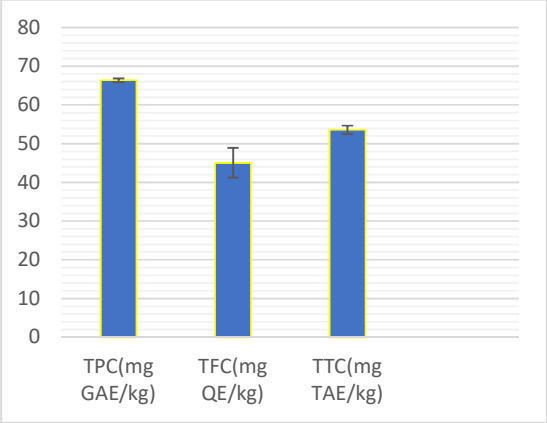

Figure 1. Evaluated total phenolic, flavonoid and tannin contents of the *C. officinalis* flower extract. Total phenolic content (TPC), Total tannin (TTC) and Total flavonoid (TFC). Values represent averages ± standard deviations for triplicate experiments.

Table1: The yield and the percentage mass of lipophilic extract of *C. officinalis*

C. officinalis	Initial mass(g)	Mass (g)	Mass (%)	Texture	Color
	100	14.32	14.32	Waxy	Dark orange

Table 2: Phytochemical screening of *C. officinalis* hexane extract. + indicates presence, − indicates absence

Phytochemical compounds	*Calendula officinalis*
Steroids	+
Terpenoids	+
Alkaloids	+
Phenols	+
Tannins	+
Flavonoids	+
Saponins	+
Glycosides	-
Reducing sugar	-
Quinones	+
Coumarins	+

3.4. GC-MS analysis

The GC-MS analysis of C**.** *officinalis* flower extract (COF) was implemented to assess the metabolite composition. The GC-MS chromatogram of the lipophilic extract is shown in Figure 2. The identification of total 24 compounds from the representing 99.15% of the total constituents (Table3).

Seven major organic classes were identified as a consequence of the lipophilic extract analysis, as illustrated in Fig.3.These classes include fatty acid (19.45%), fatty alcohol (17.54%), sesquiterpenes (34.9%), hydrocarbons (20.06%), diterpenes (3.9%), phytosterol (2.10%), and alkaloids (0.53%). One of the most prominent fatty alcohols is clearly 1-Heptatriacotanol (16.47%) followed by n-Hexadecanoic acid (5.98%), 9,12,15-Octadecatrienoic acid (omega 3) (5.55%), then 9,12-Octadecadienoic acid (omega 6) (2.35%) were the major fatty acid in this extract. In addition, many other sesquiterpene as isochiapin B and Humulane-1,6-dien-3-ol represent the major sesquiterpene compounds 15.91% and 12.96%, respectively besides other sesquiterpene Muurolol (2.1 %), α-Cadinene (2.06 %), α-Muurolene (1.4%), respectively. On the other hand, Hydrocarbons such as Octacosane (7.78%), Dotriacontane (7.78%), Eicosane (3.89) and Nonadecane (0.61%). Among the active ingredients Diterpene as Thunbergol (3.36%), phytosterol as Stigmasterol (2.10%) and alkaloid as Ethyl iso-allocholate (0.53%). Through this, it is possible to observe full scan mass spectrometric analysis of major compounds in the COF (Fig. 3 (a-f)).

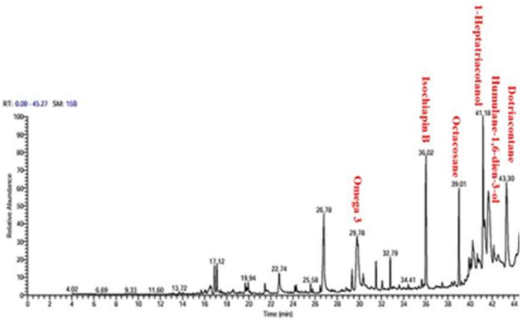

Figure 2. Gas chromatography-mass spectrometry total ion chromatogram for the lipophilic extracts from *C. officinalis*

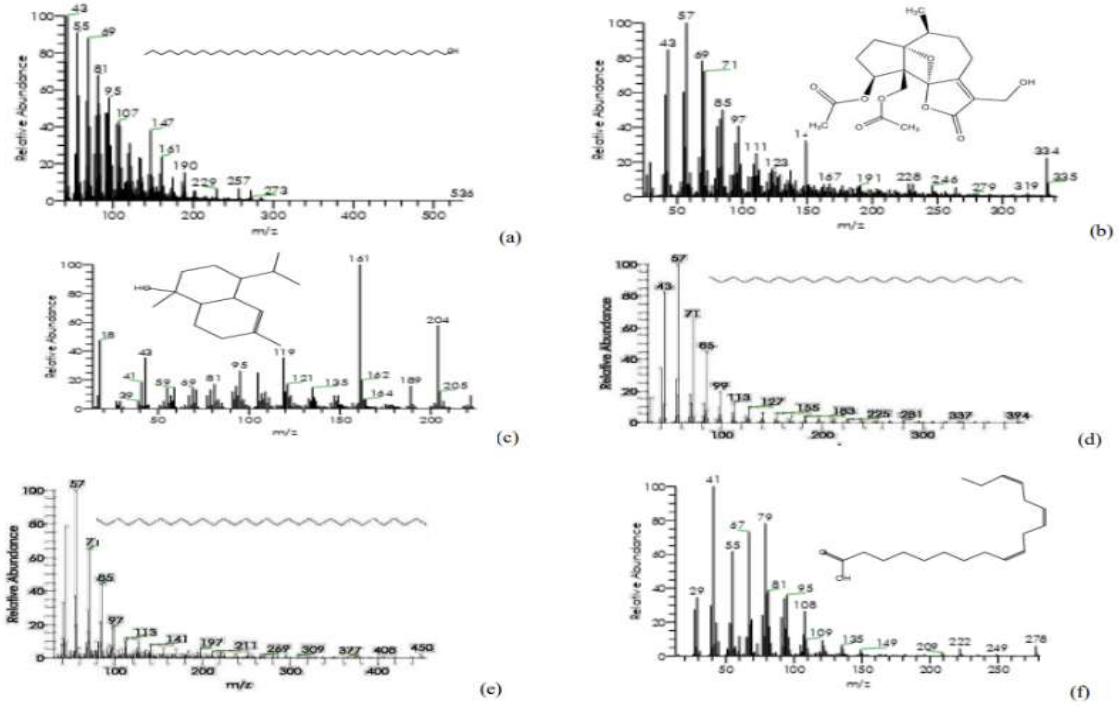

Figure 3. Gas chromatography-mass spectrometry full scan mass spectrometric analysis of compounds in the *C. officinalis* of major compounds (a) 1-Heptatriacotanol (b) Isochiapin B (c) Humulane-1,6-dien-3-ol (d) Octacosane (e) Dotriacontane (f) Omega 3 (ω3)

3.5. Evaluation of the antioxidant capacity

The 2,2-diphenyl-1-picryl-hydrazyl (DPPH), 2′azino-bis (3-ethylbenzothiazoline-6-sulfonic acid (ABTS), hydrogen peroxide (H_2O_2), and metal chelating activities of *C. officinalis* flower extract were used to assess its antioxidant capacity.

3.5.1. DPPH scavenging activity

The results revealed that hexane extract of *C. officinalis* demonstrated higher antioxidant activity 73.21± 0.22 at 160 µg/mL. The antioxidant activity of this extract showed that it depends on the amount of dose given (Figure 4a). The standard (BHT) exhibited significantly higher DPPH radical scavenging activities than those of *C. officinalis* extract. The concentrations of the studied sample extract required to scavenge 50% of the DPPH radicals (IC_{50}) were also determined in this study are shown in Table 4. The IC_{50} values for extract was 62.13± 0.37 µg/mL, However, the IC_{50} value of the standard (BHT) was 10.60±1.39 µg/mL.

3.5.2. ABTS scavenging activity

The antioxidant activity of the *C. officinalis* extract was evaluated depending on the ability to scavenge $ABTS^{\bullet+}$ radicals. The production of $ABTS^{\bullet+}$ was suppressed by the extract and the positive control Trolox in a concentration-dependent manner (Figure 4b), the results revealed that this extract demonstrated higher antioxidant activity 77.75 ± 0.45% at 160 µg/mL. The IC_{50} values for extract was 42. 18±0.35 µg/mL µg/mL, whereas, the IC_{50} value of the standard (Trolox) was 13.23 ± 1.30 µg/mL are shown in Table 4. The scavenging capacities of extract and Trolox increased gradually with increasing their concentration.

Table 3: Chemical composition and content of GC-MS analysis of fatty acids from lipophilic extracts *from C. officinalis*

No.	Retention time (min)	Compound Name	Molecular weight	Molecular Formula	Compound Type	Relative percentile
1	16.52	α-Muurolene	204	C15H24	sesquiterpene	1.4
2	17.11	α--Cadinene	204.35	C15H26	Sesquiterpene	2.06
5	19.94	T-Muurolol	222	C15H26O	Sesquiterpene	2.1
6	22.74	Tetradecanoic acid	228.4	C14H28O2	Fatty acid	2.14
7	24.16	2-Pentadecanone, 6,10,14-trimethyl-	268	C18H36O	Sesquiterpene	0.47
8	24.29	Neophytadiene	278	C20H38	Diterpene	0.54
9	25.58	Nonadecane	268	C19H40	Hydrocarbon	0.61
10	26.79	n-Hexadecanoic acid	256	C16H32O	Fatty acid	5.98
11	29.77	9,12,15-Octadecatrienoic acid(ω3)	278	C18H30O2	Fatty acid	5.55
12	29.88	9,12-Octadecadienoic acid (ω6)	298	C18H31O2	Fatty acid	2.35
13	30.34	Octadecanoic acid	284	C18H36O2	Fatty acid	0.89
14	31.50	Arachidonic acid	2.54	C20H32O2	Fatty acid	1.83
15	32.06	5,8,11,14Eicosatetraenoic acid, methyl ester	318	C21H34O2	Fatty acid ester	0.71
16	32.79	Eicosane	296	C21H44	Hydrocarbons	3.89
17	36.01	Isochiapin B	350	C19H22O6	Sesquiterpen lactone	15.91
18	39.01	Octacosane	380	C27H56	Hydrocarbons	7.78
19	39.92	Thunbergol	290	C20H34O	Diterpene alcohol	3.36
20	40.93	Ethyl iso-allocholate	436.6	C26H44O5	Alkaloid	0.53
21	41.18	1-Heptatriacotanol	537	C37H76O	Fatty alcohol	17.54
22	41.66	Humulane-1,6-dien-3-ol	222	C15H26O	Sesquiterpen	12.96
23	43.30	Dotriacontane	408	C29H60	Hydrocarbon	7.78
24	44.49	Stigmasterol	412	C29H48O	Phytosterol	2.10
%Total Identified						98.48
%Fatty acid						36.99
%Sesquiterpene						34.9
%Hydrocarbons						20.06
%Diterpene						3.9
%Phytosterol						2.10
%Alkaloid						0.53

Figure 4. Antioxidant activities (a) DPPH radical scavenging activity; (b) ABTS radical scavenging activity; (c) Hydrogen peroxide radical scavenging activity; (d) Metal chelating activity of COF in comparison to the synthetic antioxidant. Values represent averages ± standard deviations for triplicate experiments. Means with different letters indicate significant differences ($p < 0.05$).

3.5.3. Hydrogen peroxide scavenging activity (H_2O_2)

The scavenging ability of *C. officinalis* and compared with vitamin C as standards on hydrogen peroxide were determined as shown in Figure 4C. In current study, the scavenging activity values on hydrogen peroxide of 160 µg/ mL in the order of vitamin C and *C. officinalis* extract were 83.91 ±0.23% and 71.32±0.33 with IC_{50} values of 35.07± 1.83 µg/ mL and 62.79 ±1.45 µg/ mL, respectively as can be shown in Table 4.

3.5.4. Iron chelating assay

The chelation power of *C. officinalis* extract and EDTA as standard were also analyzed as shown in Figure 4D. A dose dependent increasing activity was obtained in metal chelating activity. The results observed that the hexane extract and EDTA exhibited significant capacity to chelate ferrous ions with the value of 86.00±0.51 and 93.24±0.68% at 160 µg/mL with IC_{50} values of 42.30± 0.28µg/ mL and 17.75± 1.55µg/ mL, respectively as can be shown in Table 4.

3.6. Effect of *C. officinalis* on the wound healing percentage.

Untreated wound group showed a non-healed contracted wound after 10 days, whereas, topical application with *C. officinalis* 2.5% and 5% for 10 days, ameliorated wound by 92% and 96%, respectively, as compared to untreated group. *C. officinalis* 5% treatment had wound closure near to normal rats (Figures 5 a and b).

3.7. Effect of *C. officinalis* on oxidative stress in wound healing model

As shown in Figure 6, wound incision-induced oxidative stress evidenced by increase of DPPH by 90%, ABTS by 81% and hydrogen peroxide radicle by 60% as compared to normal rats *C. officinalis 2.5% and 5%* had scavenging activity values on DPPH by 5.5-fold and 10 fold, ABTS by 3.9 fold and 4.2 fold, as compared to wounded group skin homogenate. In the same time *C. officinalis 2.5% and 5%* had antioxidant *against* hydrogen peroxide radicle by 1.2fold and 1.4-fold, respectively, as compared to wounded group skin homogenate.

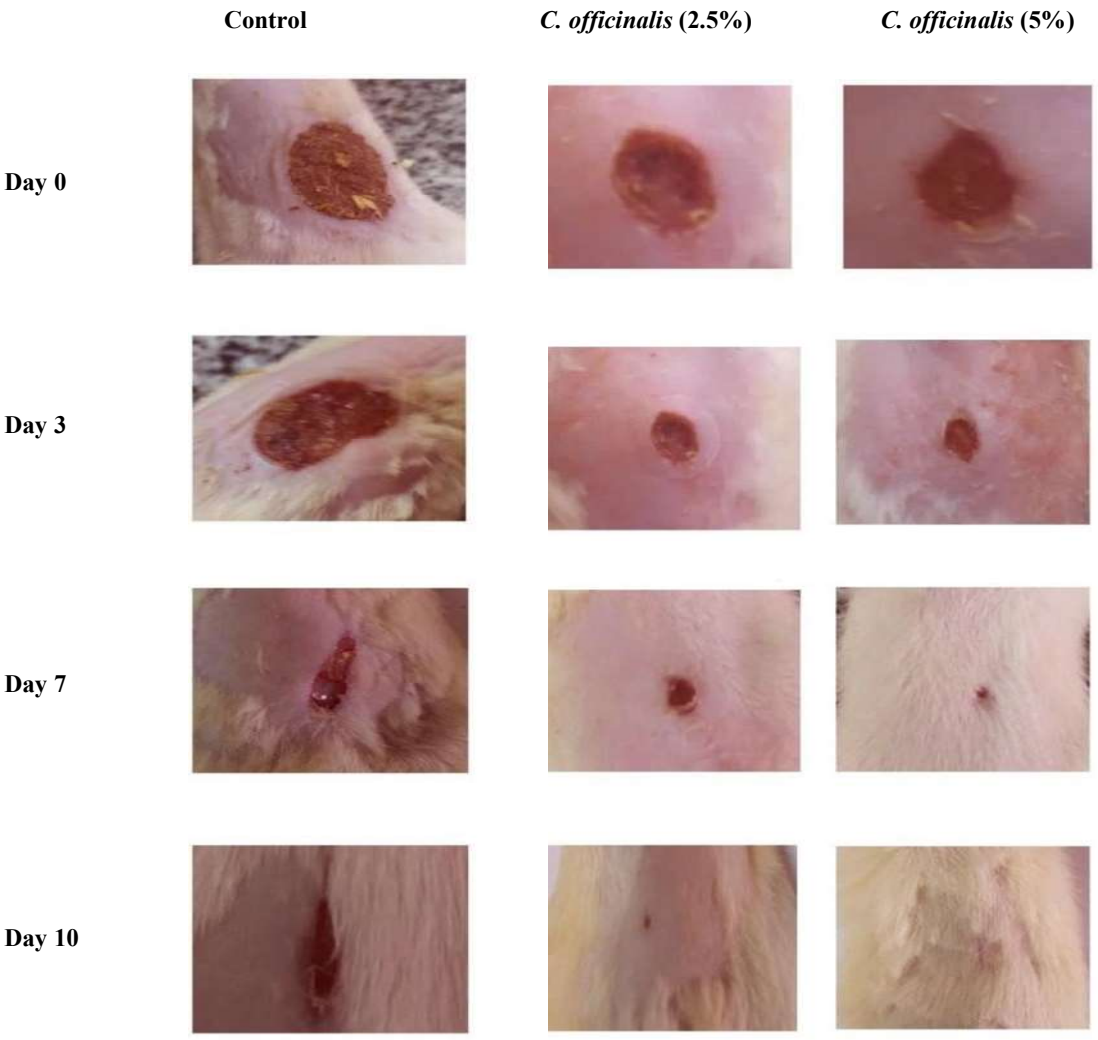

Figure 5a. Macroscopic morphology of the healing progress of *C. officinalis* at 0-, 3-, 7- and 10-days post wounding

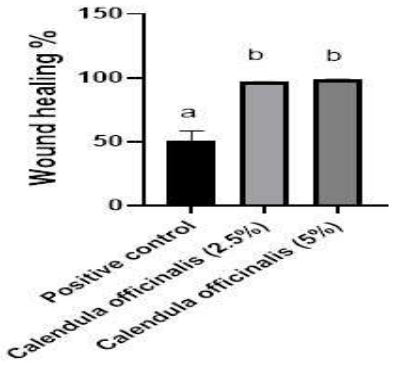

Figure 5b. Effect of *C. officinalis* on the wound healing %

Data are presented as the mean ± SD (n=6) for each group. Statistical analysis was conducted by ANOVA followed by Fisher's LSD comparisons test. Same letter means non-significant difference, while different letter means significant difference at $p < 0.05$.

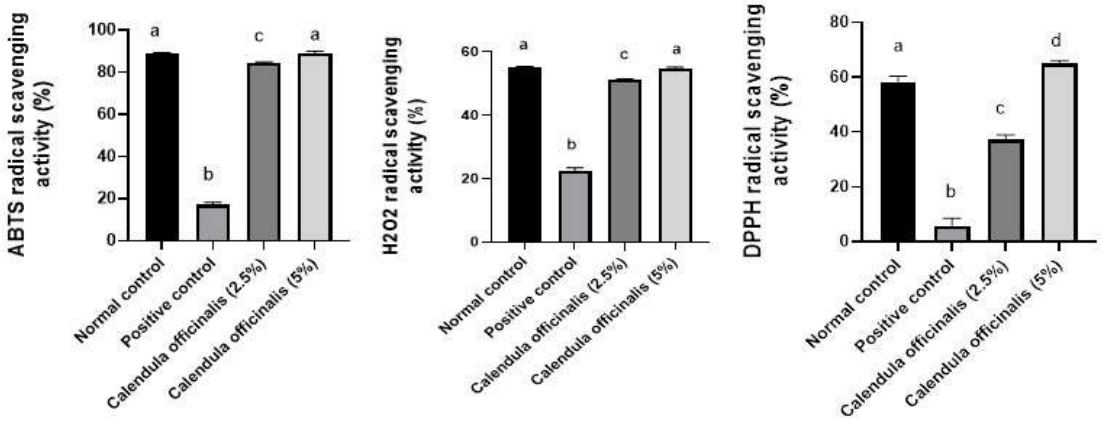

Figure 6. Effect of *C. officinalis* on oxidative potential (ABTS, H_2O_2 and DPPH radical scavenging activities) in wound healing model.

Data are presented as the mean ± SD (n=6) for each group. Statistical analysis was conducted by ANOVA followed by Fisher's LSD comparisons test. Same letter means non-significant difference, while different letter means significant difference at $p < 0.05$.

Table 4: Concentrations necessary for 50% antioxidant inhibition (IC50) (A) DPPH; (B) ABTS;(C) hydrogen peroxide; (D) metal chelating activity of *C. officinalis* in comparison to the synthetic antioxidant. Statistical analysis was conducted by ANOVA followed by Fisher's LSD comparisons test Significantly different from standard at p<.05.

Material	IC_{50}/µg/ml (DPPH) `	IC_{50}/µg/ml (ABTS)	IC_{50}/µg/ml (H_2O_2)	IC_{50}/µg/m (Metal chelating activity)
C. officinalis	62.13± 0.37 [b]	42. 18±0.35 [b]	62.79±1.45 [b]	42.30± 0.28[b]
BHT Standard	10.60±1.39 [a]	--	--	--
Trolox Standard	--	13.23 ± 1.30 [a]	--	--
VIT C Standard	--	--	35.07± 1.83 [a]	--
EDTA Standard	--	--	--	17.75± 1.55[a]

Note: Each data represents the mean± SD of three independent experiments where means with different letters in the same column indicate significant differences ($p < 0.05$).

3.8. Effect of *C. officinalis* on the expression of collagen, MMP9, AMPK and HIF-1α in wound healing model

In current study, collagen was significantly decreased in rats exposed to wound by 59% with an elevation in MMP9 levels by 175 %, as compared with normal control group. Topical application with *C. officinalis* 2.5% and 5% for 10 days elevated the skin content of collagen by 59% and 127% respectively, and decreased MMP9 by 39% and 55%, respectively, as compared to wounded group. In addition, treatment with *C. officinalis 5%* treatments returned the levels of collagen and MMP9 to their normal values (Figures 7a and b).

AMPK was significantly decreased in rats exposed to wound by 38%, as compared with normal control group Topical application with C. *officinalis 2.5% and 5%* for 10 days elevated the levels of AMPK by 25% and 60% respectively, as compared to control positive group, moreover, the treatment with *C. officinalis 5%* returned it to normal level (Figure 7c). Moreover, HIf1α was significantly decreased in rats exposed to wound by 53% as compared with normal control group. Topical application with C. *officinalis 2.5% and 5%* for 10 days increased the levels of HIf-1α by 38% and 69% respectively, as compared to control positive group. In addition, the treatment with *C. officinalis 5%* returned it to normal level (Figure 7d).

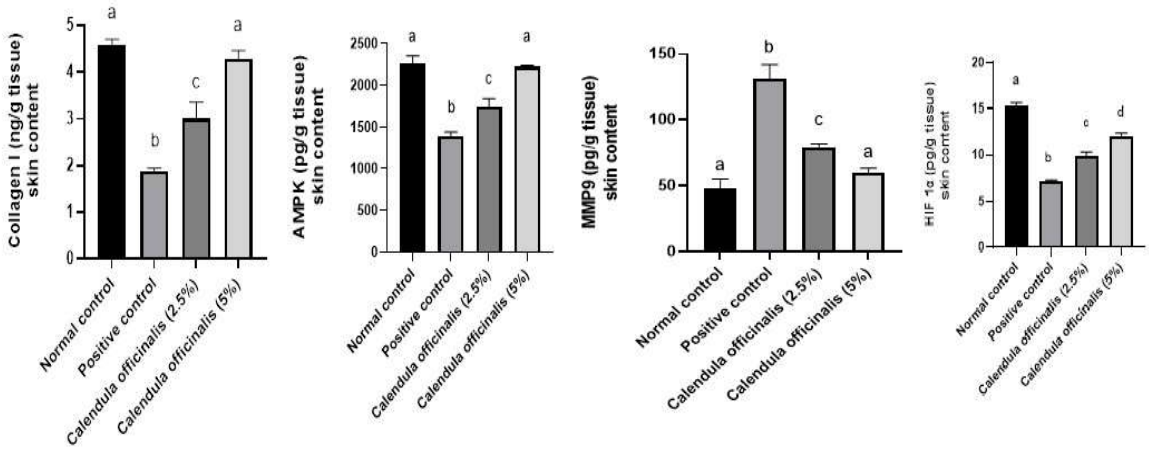

Figure7. Effect of *C. officinalis* on the expression of collagen, AMPK, MMP9, HIF-1α in wound healing model.
Data are presented as the mean ± SD (n=6) for each group. Statistical analysis was conducted by ANOVA followed by Fisher's LSD comparisons test. Same letter means non-significant difference, while different letter means significant difference at $p < 0.05$.

3.9. Histopathological Findings

Normal rats showed no histopathological alteration and the normal histological structure of the epidermis, dermis with hair follicles and sebaceous glands and subcutaneous tissue were recorded in Figures 8a and b. While experimentally inducted rats (wound) exhibited Focal ulceration and necrosis were detected in the superficial layers of epidermis and dermis with massive inflammatory cells aggregation (Figure 8c). Granulation tissue formation with inflammatory cells infiltration were detected in the deep dermal layer (Figure 8d). The subcutaneous tissue showed oedema and inflammatory cells infiltration (Figure 8e). Treatment with low dose of *C. officinalis* showed intact epidermis and underlying dermis with hair follicles and sebaceous glands (Figure 8f). Oedema and inflammatory cells infiltration with granulation tissue formation were detected in the deep layer of dermis (Figure 8g). There were oedema and inflammatory cells infiltration in the subcutaneous tissue (Figure 8h). Also, high dose of *C. officinalis* showed intact dermis with hair follicles and sebaceous glands (Figure 8i). There was intact musculature (Figure 8j) while the underlying subcutaneous tissue showed few oedema and inflammatory cells infiltration (Figure 8k).

3.10. Molecular docking

The DFT B3LYP/6-31G (d,p) optimized structures of 1-heptatriacotanol and isochiapin B are shown in Fig. 9. Table 5 demonstrates the resulting values of binding affinity of 1-heptatriacotanol and isochiapin B with the designated proteins.

Figure 10 demonstrates the docked complexes of 1heptatriacotanol with AMPK, collagenase, HIF-1α, MMP-9, TNF-α, and VEGF, displaying the orientation of the ligand, the sites of interaction and the key amino acid residues of each protein involved in interaction. The 2D diagrams of the amino acid residues of each protein interaction with 1-heptatriacotanol are shown in Figure 11.

Demonstrated in Figure 12 are the docked complexes of isochiapin B with AMPK, collagenase, HIF-1α, MMP-9, TNF-α, and VEGF. Figure 13 represents the 2D diagrams of the amino acid residues of each protein's interaction with isochiapin B. The active site residues of AMPK, collagenase, HIF-1α, MMP-9, TNF-α, and VEGF involved in hydrogen bond interaction with isochiapin B are listed in Table 6.

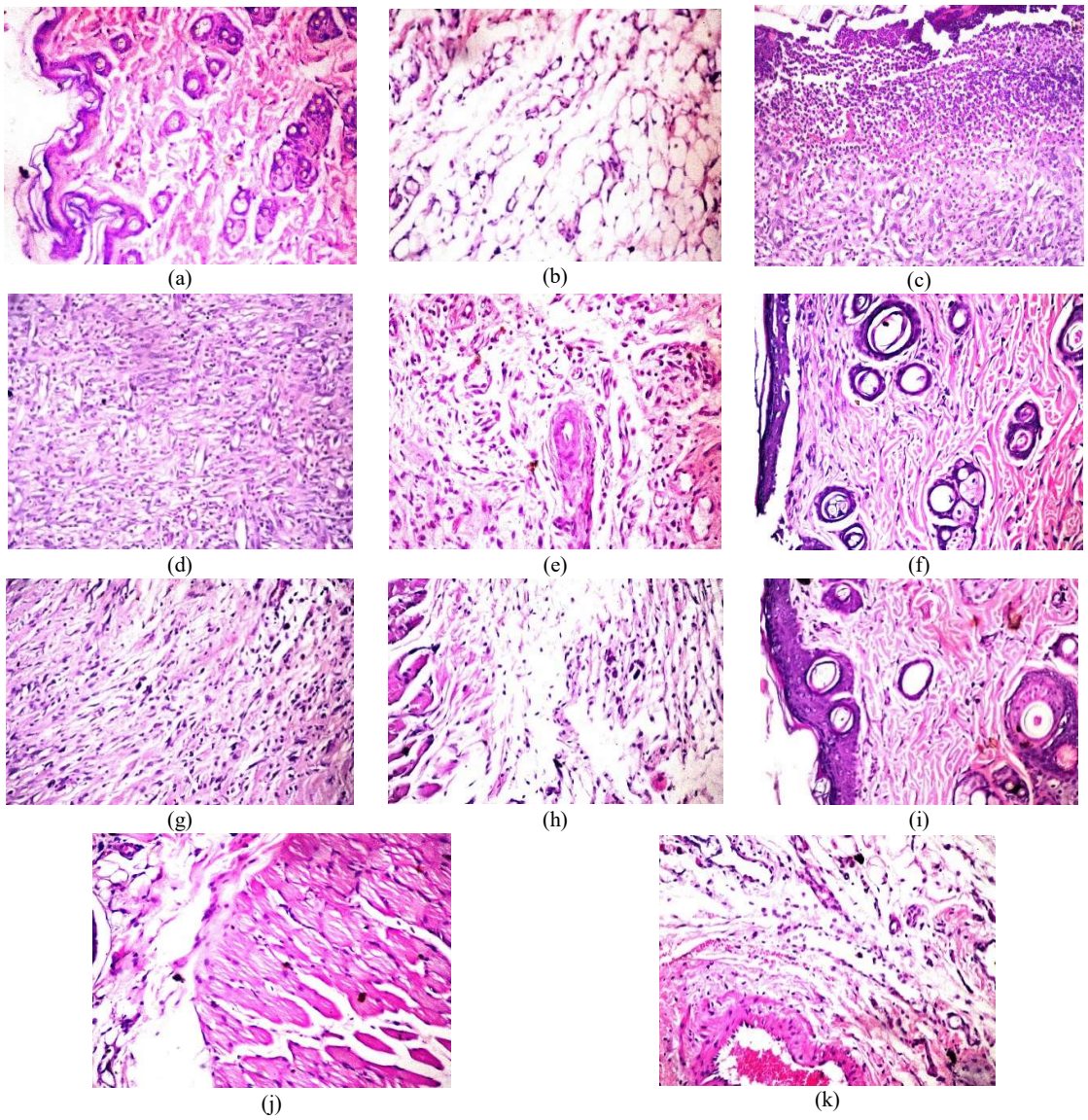

Figure 8. Histopathological Findings of skin.

Normal rats showed no histopathological alteration and the normal histological structure of the epidermis, dermis with hair follicles and sebaceous glands and subcutaneous tissue were recorded in (Fig. a & b). While experimentally inducted rats (wound) exhibited Focal ulceration and necrosis were detected in the superficial layers of epidermis and dermis with massive inflammatory cells aggregation (Fig. c). Granulation tissue formation with inflammatory cells infiltration were detected in the deep dermal layer (Fig. d). The subcutaneous tissue showed oedema and inflammatory cells infiltration (Fig. e). Treatment with low dose of C. officinalis showed intact epidermis and underlying dermis with hair follicles and sebaceous glands (Fig. f). Oedema and inflammatory cells infiltration with granulation tissue formation were detected in the deep layer of dermis (Fig. g). There were oedema and inflammatory cells infiltration in the subcutaneous tissue (Fig. h). Also, high dose of C. officinalis showed intact dermis with hair follicles and sebaceous glands (Fig. i). There was intact musculature (Fig. j) while the underlying subcutaneous tissue showed few oedema and inflammatory cells infiltration (Fig. k).

Tabel 5: Binding affinities of 1-heptatriacotanol and isochiapin B with AMPK, collagenase, HIF-1α, MMP-9, TNF-α, and VEGF.

Protein	Binding affinity (kcal/mol)	
	1-Heptatriacotanol	Isochiapin B
AMPK	-2.11	-8.51
Collagenase	-3.47	-8.31
HIF-1α	-5.5	-8.13
MMP-9	-3.26	-9.15
TNF-α	-5.2	-7.91
VEGF	-2.31	-7.84

Table 6: Active site residues of AMPK, collagenase, HIF-1α, MMP-9, TNF-α, and VEGF involved in hydrogen bond interaction with isochiapin B.

Protein	Active site residues involved in hydrogen bond interaction
AMPK	Arg152, Thr168, Lys170
Collagenase	Asn180, Ala182, Tyr240
HIF-1α	His199, Gln239, His279
MMP-9	Leu188, His401, Glu402, His411
TNF-α	Ser60, Leu120
VEGF	Asn62, Asp63, Glu64, Lys107

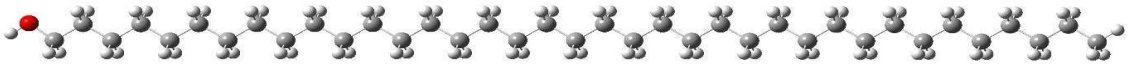

1-Heptatriacotanol

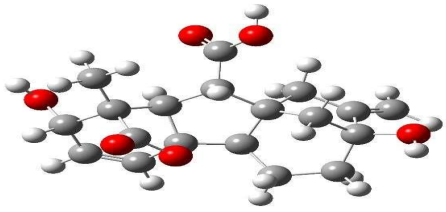

Figure 9. B3LYP/6-31G (d,p) optimized structures of the compounds 1-Heptatriacotanol and Isochiapin B

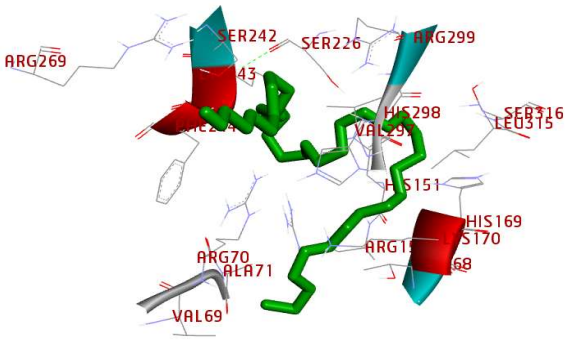

AMPK

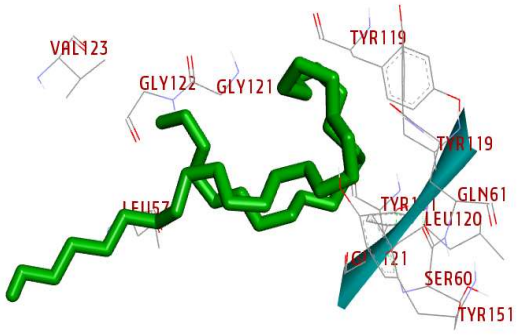

TNF-α

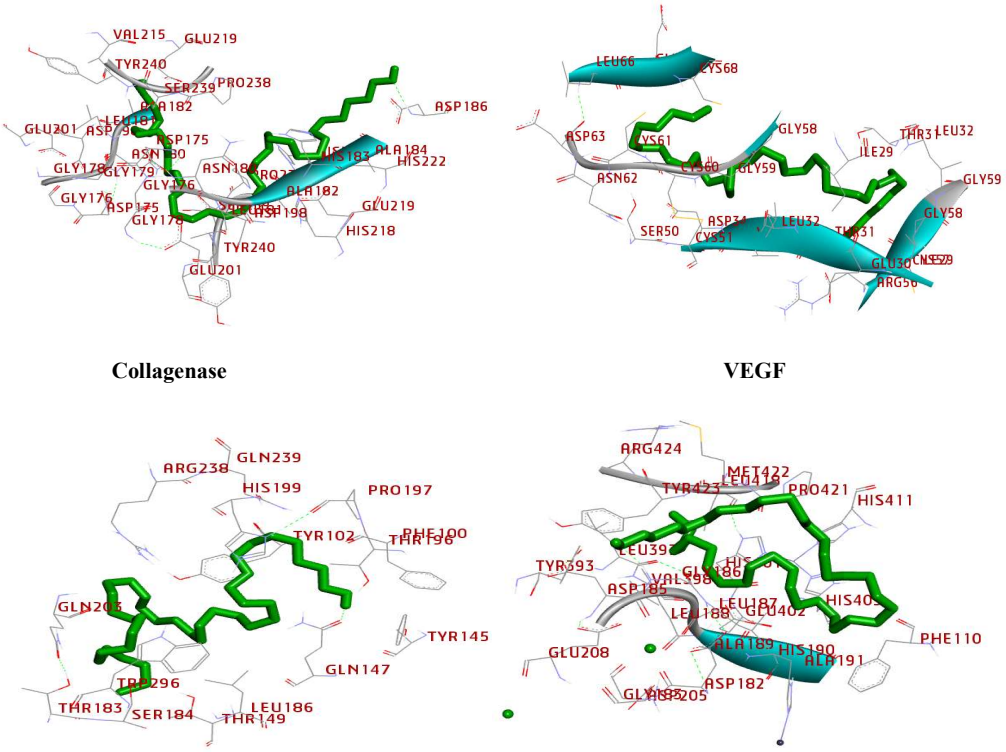

Figure 10. 3D view of the docked 1-Heptatriacotanol with AMPK, collagenase, HIF-1α, MMP-9, TNF-α, and VEG

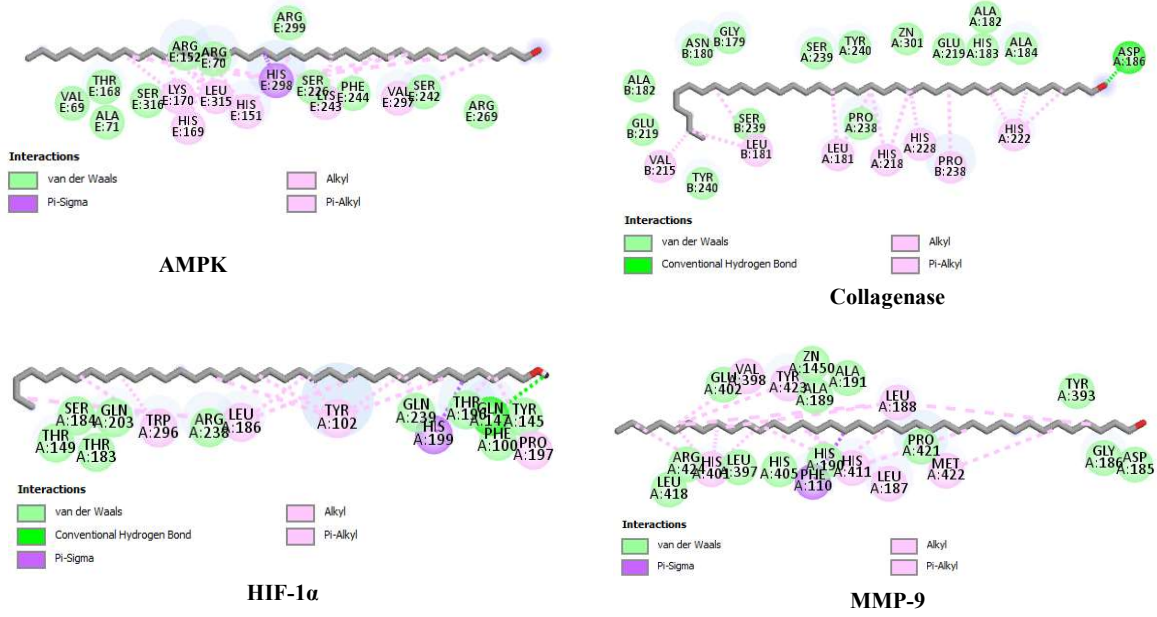

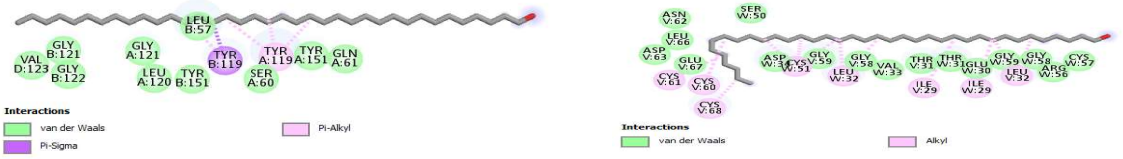

TNF-α **VEGF**

Figure 11. 2D diagrams of amino acid residues of AMPK, collagenase, HIF-1α, MMP-9, TNF-α, and VEGF interacting with 1-Heptatriacotanol, showing bond types.

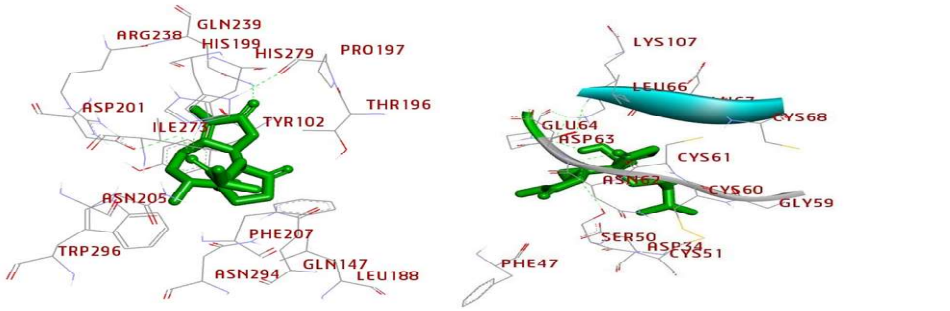

HIF-1α **VEGF**

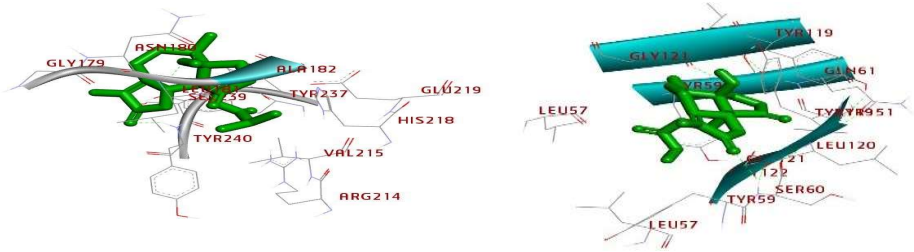

Collagenase **TNF-α**

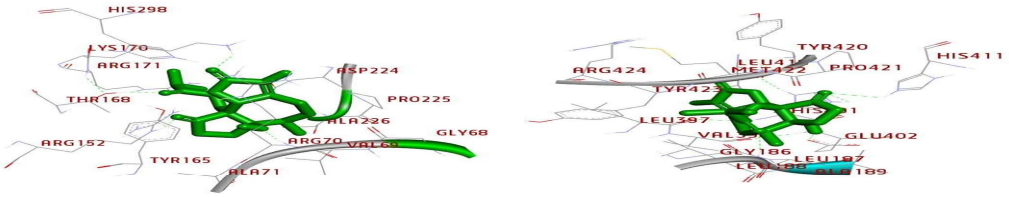

AMPK **MMP-9**

Figure 12. 3D view of the docked Isochiapin B with HIF-1α, VEGF, collagenase, TNF-α, AMPK and MMP-9.

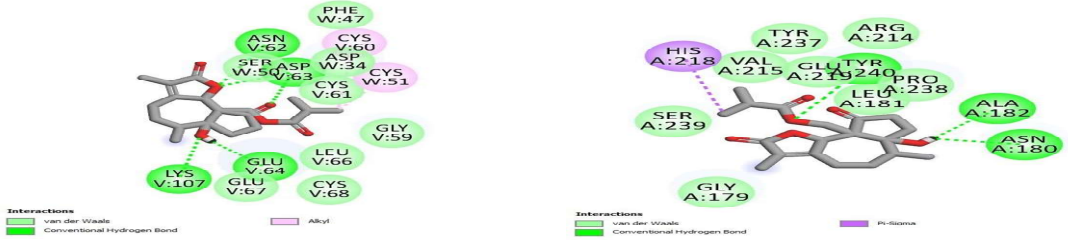

VEGF **Collagenase**

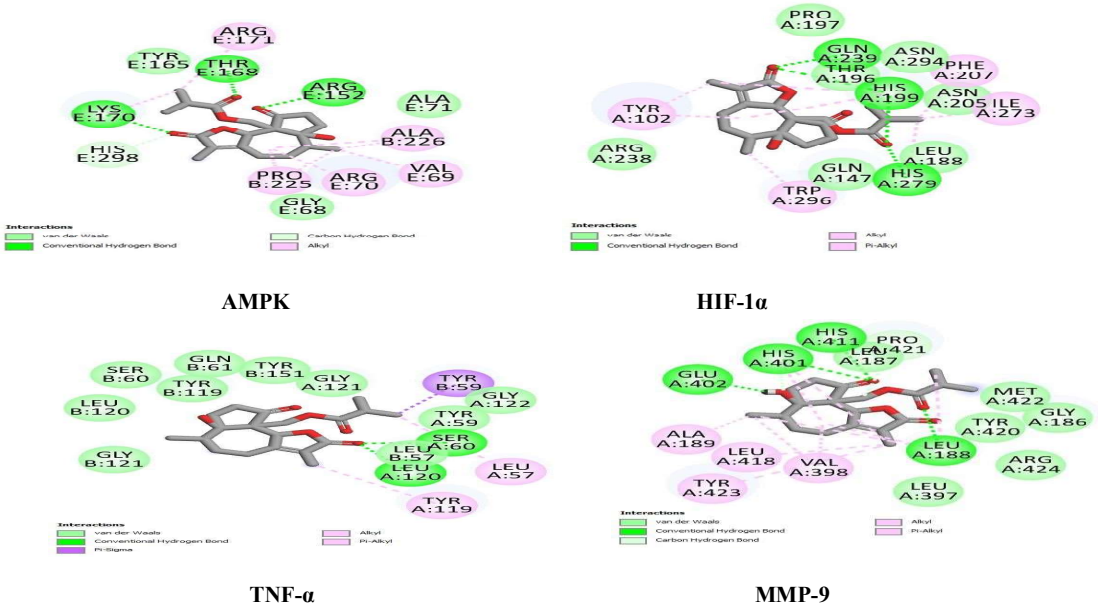

Figure 13. 2D diagrams of amino acid residues of VEGF collagenase, AMPK, HIF-1α, TNF-α and MMP-9, interacting with Isochiapin B, showing bond types.

4. Discussion

Healing wound is integrated sequence of events that involves the intricate interplay of immune cells, cytokines, growth factors, and injured skin cells with tissue sequences like angiogenic responses, cellular migration, proliferation, and wound tissue fibroplasia. ROS production is crucial to both healthy physiology and the development of many diseases. Oxidative stress might influence the stages of wound healing [53]. An epidemiological study showed that the frequency of wounds resulting from various causes is steadily rising, and annual medical expenses are also rising [54]. Our results exhibited that wound incision induced oxidative stress evidenced by increase of DPPH, ABTS and hydrogen peroxide radicle in the skin as compared to normal rats. Moreover, wound incision decreased the skin content of collagen. The formation of the extracellular matrix (ECM) through collagen and α-smooth muscle actin (α-SMA) is promoted by TGF-β1 and VEGF which are included in healing process via cell proliferation angiogenesis and re-epithelialization [37]. The shrinkage of the wound depends on contractile microfilament bundles known as "myofibroblasts," which are generated by fibroblasts during the healing process. The expression of α-SMA characterizes the fully differentiated myofibroblast. Keratinocytes are also thought to be important cells in the contraction and healing of skin wounds [55]. MMP-9 is an important molecular expression pattern of wound healing-related genes that possesses main role in extracellular matrix proteins degradation during organogenesis as well as normal tissue turnover [56]. Wounded rats in current study suffered from an elevation in MMP9 which may delay wound healing. Furthermore, Huang et al. [57] have found that HIf-1α is a downstream element of AMPK which stimulates its pro-angiogenic effects modulating ROS.HIF-1α, in the same time, upregulates tissue expression of VEGF, which in turn promote an angiogenic response [58]. Our results revealed that wound incision provokes decrease in AMPK and HIF1α inhibiting angiogenic process. *C. officinalis* has grab more attention as a result of its antioxidant and anti-inflammatory qualities, and has benefits as a food additive and for use in cosmetic and biomedical applications [59]. Our results support earlier research by Fronza et al. [60] found that hexane extract from *C. officinalis* stimulated proliferation and migration of fibroblasts at low concentrations. Additionally, our findings are in accordance with European Medicines Agency (EMA) which certified its lipophilic and aqueous alcoholic extract in the treatment of minor skin inflammation and wounds healing [13]. The most widely used screening techniques for medicinal plants and in silico screening often contain a large number of bioactive phytocompounds and phytochemicals. Identification of the bioactive compounds responsible for activity and/or reaction mechanisms is made more challenging by this multi-composition state. Therefore, appropriate methods for identifying bioactive compounds from medicinal plants are developed with the aid of phytochemical and in silico bioactivity screening procedures [61].

GC-MS and in silico screening tools for pharmacokinetic and pharmacodynamic property

prediction are examples of phytochemical screening tools. The screening for phytochemicals revealed the presence of terpenoids, steroids, phenols, flavonoids, tannins , saponins , alkaloids, quinones and coumarins may be the reason for *C. officinalis* extract biological activities [62]. Minor differences were observed in our study and previous one conducted on *C. officinalis* methanolic extract of the phytochemical screening. The variation may result from variations in genetic, carcinogenic, morphogenetic, environmental, and other factors, as well as from environmental adaptation, organism's interaction and history evolution [63]. In addition, the total phenolic, flavonoid and tannin were found in *C. officinalis* hexane extract. Phenolic compounds are well known for their ability to chelate redox-active metal ions and stop hydroperoxides from becoming reactive oxyradicals, which can then inactivate free radical [64]. Flavonoids' capacity to both scavenge and inhibit the production of free radicals contributes to their antioxidant activity [65]. On the other hand, Rigane et al. [66] reported different total phenolic and flavonoid values for various parts of the plant as aqueous methanol flower and leaves. The differences between our results and other investigators may be related to the polarity of the solvents [67].

GC–MS analysis revealed the presence of 24 compounds. The phytochemical analysis exhibited seven main different organic classes were identified as fatty acid, fatty alcohol sesquiterpene, hydrocarbons, diterpene, phytosterol and alkaloid. Most of the identified compounds belonged to fatty alcohol among which1-Heptatriacotanol is the major fatty acid compounds followed by n-Hexadecanoic acid, 9,12,15-Octadecatrienoic acid (omega 3), then 9,12-Octadecadienoic acid (omega 6). In addition, many other sesquiterpene as isochiapin B and Humulane-1,6-dien-3-ol represent the major sesquiterpene compounds. A A previous work studied different of phyto-constituents as GC–MS analysis in four taxa of this genus as C. officinalis, C. suffruticosa, C. arvensis and C. suffruticosa hexane extract [68]. Different secondary metabolites may be produced in different parts of medicinal plants through unique regulatory pathways and unique transport routes according to complexity of phytochemicals as well as diversity of the plant parts [63]. Specific tissues and developmental phases have an impact on the phytochemical biosynthesis-related gene expression pattern [62]. Antioxidant activity is a crucial quality requirement for medicinal plants. Several in vitro antioxidant methodologies can be used to determine antioxidant activity. A single assay cannot accurately determine antioxidant capacity because each has advantages and disadvantages of its own. It was crucial to evaluate the antioxidant capacity in the current study employing DPPH, ABTS, H_2O_2, and metal-chelating assays. Antioxidants protect cells from the potential damage that an excess of ROS can cause by neutralizing reactive species and halting oxidation processes. Antioxidant properties are included in several of *C. officinalis* extract naturally occurring components. The *C. officinalis* flower hexane extract obtained in this study has a significant antioxidant property in all assays. Other result supported by AK et al. [69] found flower extracts of *C. officinalis* exhibited stronger ability when compared to roots, on the other hand *C. officinalis* leaf extracts showed highest chelating activity and further support the antioxidant capacity of formulations prepared with *C. officinalis* flowers by Venkatesh et al. [70]. The antioxidant capacity in *C. officinalis* flower hexane extract might be due to the high content of phytochemical constituents which may be the reason for wound healing properties, *in vivo* study, that it acts as a scavenger of ROS in skin evidenced by inhibition of DPPH, ABTS and hydrogen peroxide [71] and increased the synthesis of collagen in wounded skin. These results suggest its beneficial effect on cutaneous wound healing due to their fatty acid content and sesquiterpene lactone. 1-Heptatriacotanol fatty alcohol has antioxidant and anti-inflammatory [72]. Additionally, other studies showed wound healing activity of Omega-3 which has been shown to aid fibroblasts in synthesizing collagen and modulate initial phases of wound healing [73,74]. Furthermore, sesquiterpene lactone isochiapin B possess antioxidant activity, anti-inflammatory and promotes wound healing [75,76]. The phytochemical analysis confirmed the presence of the sesquiterpenes which may be the reason for the efficiency of C. *officinalis* in healing wounds through elevated rate of wound contraction, cellular proliferation, granulation tissue formation, and collagen synthesis. Stigmasterol, or phytosterol, another significant component of *C. officinalis*, lowers the generation of ROS [77,78]. *In vitro* studies of stigmasterol reduced the release of pro-inflammatory mediators [79]. Alkaloid as ethyl iso-allocholate, also, possess antioxidant properties [80] and promotes the wound healing process [81].

C. officinalis, in current work, reduced MMP-9 inhibiting ECM degradation. These findings may be due to the presence of octacosane and eicosane that promote wound healing due to their potent free radical scavenging and possible interactions with MMP-9 [82]. This result could also be due to the presence of isochiapin B since it has also been reported that isochiapin B has antioxidant activity and promotes wound healing [75,83]. In a previous work, *C. officinalis* reduced MMP-9 levels and stimulated angiogenesis in a localized wound of diabetic animals [11]. Belal et al. [2] have previously reported on in silico MMP9 inhibitor efficacy of the constituents of Calendula extract in comparison to RND-336 as a well-known MMP-9 inhibitor. Their results indicated

that the highest potency against MMP-8 and MMP-9 were attributed to the structures comprising the benzopyran4-one moiety, thus concluding that Calendula extract has a potential role in wound healing via inhibiting both enzymes. *C. officinalis* administration, in this study, for the first-time elevated AMPK and HIF-1α which in turn enhances the synthesis of angiogenesis. These results supported by our histopathological examination that revealed inhibition of inflammatory cell infiltration and stimulation of wound contraction, epithelialization, angiogenesis, and ECM deposition in *C. officinalis* group as compared to positive control group. Previously, *C. officinalis* flower exhibited an elevation of VEGF expression levels in C57BL/6 mice lung metastasis [84]. Molecular docking results showed that the general case is that isochiapin B had better binding affinities than 1-Heptatriacotanol in the interaction with AMPK, Collagenase, HIF-1α, MMP-9, TNF-α, and VEGF.The best binding affinity of 1-Heptatriacotanol was for its interaction with HIF-1α with an affinity score of 5.5 kcal/mol, while the least binding affinity was for its interaction with AMPK with the affinity score of - 2.11 kcal/mo.

The 2D diagrams of 1-Heptatriacotanol's interactions with the proteins indicated that all the interactions are stabilized by van der Waals interactions as well as hydrophobic interactions in the form of alkyl and mixed Pi/Alkyl hydrophobic interactions. The presence of hydrogen bonds was only noticed in the interaction of 1Heptatriacotanol with collagenase and with HIF-1α. In the interaction with collagenase, a hydrogen bond was formed between the oxygen atom of the terminal hydroxyl group of 1-Heptatriacotanol and Asp168 amino acid residue, while in the interaction with HIF1α the hydrogen bond was formed with Gln147 amino acid residue [85]. On the other hand, the best binding affinity of isochiapin B was for its interaction with MMP-9, with an affinity score of -9.15 kcal/mol, while the least binding affinity was for its interaction with VEGF with an affinity score of -7.84 kcal/mol. This result is in agreement with the results of free radical scavenging activity of *C. officinalis* extract and its possible interactions with MMP-9. The 2D diagrams of isochiapin B interactions with the proteins confirmed that the interactions are stabilized by more hydrogen bonds than in the case of 1-Heptatriacotanol, which explains the significantly enhanced binding affinities of isochiapin B to the designated proteins compared to 1-Heptatriacotanol, since hydrogen bonds are key interactions in enhancing the protein ligand binding affinity [86].

Conclusion

C. officinalis treatment has a potent antioxidant effect and elevates collagen fibrous protein which essentially contributes to wound strength. It inhibits the inflammatory processes and degradation of extracellular matrix (ECM) via decreasing MMPs with stimulation AMPK and HIF-1α. *C. officinalis* may be used as a biomedical skin wounds agent to treat scar formation.

Conflicts of interest

On behalf of all authors, the corresponding author states that there is no conflict of interest.

Funding

No funds, grants, or other support was received for conducting this study.

Ethical approval

All animal experiments met the standards of the Animal Ethics Committee of National Research Centre, Egypt and were reviewed and approved by the Medical Research Ethics Committee at the National Research Centre, Egypt (Reg. No. 2445062022). We confirm that the study complies with the ARRIVE guidelines [(https://arriveguidelines.org).] and we confirm that all methods were performed in accordance with the relevant guidelines and regulations.

Credit authorship contribution statement

A.S. Conceptualization, Methodology, Formal analysis, Investigation, Resources, Writing, Review and editing the manuscript. M.I.E. Corresponding author, Methodology, Resources, Writing - original draft, Revising and editing the manuscript. A.R. Performed molecular docking simulation and analysis, writing docking part, Revising and editing the written manuscript. R.M.M.M. Conceptualization, Methodology, Formal analysis, Resources, Writing - original draft, Revising and editing the written manuscript. All authors approved the final version of the manuscript.

References:

[1] Agwa, M. M., El-Aassar, M. R., Moustafa, R. I., Elsayed, H., El-Beheri. N. G., 2024. Rapid RPHPLC detection method for quantification of gentamicin sulfate loaded wound dressing nanofiber formulation with accelerated in Vivo wound healing. *Egypt. J. Chem.* 67(6), 445 – 456.

[2] Belal, A., Elanany, M. A., Raafat, M., Hamza, H. T. & Mehany, A. B. M., 2022. Calendula officinalis Phytochemicals for the Treatment of Wounds Through Matrix Metalloproteinases-8 and 9 (MMP-8 and MMP-9): In Silico Approach. Nat. Prod. Commun. 17(5), 1–16.

[3] Boateng, J. S., Matthews, K. H., Stevens, H. N. & Eccleston, G. M., 2008. Wound healing dressings and drug delivery systems: a review. *J. Pharm. Sci.* 97(8), 2892–2923.

[4] Aly, F. U., Abou-Taleb, H. A., Abdellatif, A. A. & Sameh Tolba, N., 2019. Formulation and evaluation of simvastatin polymeric nanoparticles loaded in hydrogel for optimum wound healing purpose. *Drug Des. Devel. Ther.* 13, 1567–1580.

[5] Peña, O. A. & Martin, P., 2024. Cellular and molecular mechanisms of skin wound healing. *Nature Reviews Molecular Cell Biology* 25, 599–616.

[6] Mohanty, C., Das, M. & Sahoo, S. K., 2012. Sustained wound healing activity of curcumin loaded oleic acid based polymeric bandage in a rat model. *Mol. Pharm.* 9(10), 2801–2811.

[7] Omura, J. Satoh, K., Kikuchi, N., Satoh, T. & Kurosawa, K., *et al.,* 2016. Protective Roles of Endothelial AMP-Activated Protein Kinase Against Hypoxia-Induced Pulmonary Hypertension in Mice. *Circ. Res.* 119(2), 197– 209.

[8] Li, F. Y. Lam, S., L., Tse, H., Chen C., & Wang, Y., *et al.,* 2012. Endothelium-selective activation of AMP-activated protein kinase prevents diabetes mellitus-induced impairment in vascular function and reendothelialization via induction of heme oxygenase-1 in mice. *Circulation* 126(10), 1267–1277.

[9] Lin, J. T., Chen, H. M., Chiu, C. H. & Liang, Y. J., 2014. AMP-activated protein kinase activators in diabetic ulcers: from animal studies to Phase II drugs under investigation. *Expert Opin. Investig. Drugs* 23(9), 1253–1265.

[10] Abdel Malik, R. Zippel, N., Frömel, T., Heidler, J., & Zukunft S., et al., 2017. AMP-Activated. Protein Kinase α2 in Neutrophils Regulates Vascular Repair via Hypoxia-Inducible Factor-1α and a Network of Proteins Affecting Metabolism and Apoptosis. Circ. Res. 120(1), 99–109.

[11] Ashwlayan, V. D., Kumar, A., Verma, M., Garg, V. K. & Gupta, S. K., 2018. Therapeutic Potential of *Calendula officinalis*. *Pharm. Pharmacol. Int. J.* 6(2), 149–155.

[12] Givol, O. Rachel Anne Kornhaber, D., V., Cleary, M., Visentin, D., C., & Haik, J. M., et al. 2019. A systematic review of *Calendula officinalis* extract for wound healing. *Wound Repair Regen.* 27(5), 548–561.

[13] Nicolaus, C. Junghanns, S., Hartmann, A., Murillo, R., Ganzera, M., *et al.,* 2017. In vitro studies .to evaluate the wound healing properties of *Calen dula officinalis* extracts. *J. Ethnopharmacol.* 196, 94–103.

[14] Pedram Rad, Z., Mokhtari, J. & Abbasi, M., 2019. Preparation and characterization of *Calendula officinalis*-loaded PCL/gum arabic nanocomposite scaffolds for wound healing applications. *Iran. Polym. J.* 28, 51–63.

[15] Lima, A. M. Siqueira, A. S., Saraiva, M. L., Möller, M. L. S., & Cruz, J. N., *et al.,* 2022. *In silico* improvement of the cyanobacterial lectin microvirin and mannose interaction. *J. Biomol. Struct. Dyn.* 40(3), 1064–1073.

[16] Bharatan, V., 2008. Homeopathy and systematics: a systematic analysis of the therapeutic effects of the plant species used in homeopathy. *Homeopathy* 97(3), 122–128.

[17] Ukiya, M. Akihisa, T., Yasukawa, K., Tokuda, H., & Suzuki T., *et al.,* 2006. Antiinflammatory, anti-tumor-promoting, and cytotoxic activities of constituents of marigold (*Calendula officinalis*) flowers. *J. Nat. Prod.* 69(12), 1692–1696.

[18] Singh, M. & Bagewadi, A., 2017.Comparison of effectiveness of *Calendula officinalis* extract gel with lycopene gel for treatment of tobaccoinduced homogeneous leukoplakia: A randomized clinical trial. *Int. J. Pharm. Investig.* 7(2), 88–93.

[19] Mehta, D., Rastogi, P., Kumar, A. & Chaudhary, A. K. 2012. Review on Pharmacological Update: *Calendula Officinalis* Linn. *Inventi*, 195–203.

[20] Ibrahim SA. & Li SK., 2010. Efficiency of fatty acids as chemical penetration enhancers: Mechanisms and structure enhancement relationship. *Pharm. Res.*; 27**:**115–125.

[21] Tu, P. T. B, & Tawata S., 2015.Anti-oxidant, antiaging, and anti-melanogenic properties of the essential oils from two varieties of *Alpinia zerumbet*. *Molecules*.; 20:16723–16740.

[22] Ijaz M, & Akhtar N., 2020. Fatty acids based αTocopherol loaded nanostructured lipid carrier gel: In vitro and in vivo evaluation for moisturizing and anti-aging effects. *J. Cosmet. Dermatol*; 19:3067–3076.

[23] Salem M, A., Manaa, E. G., Osama, N., Aborehab, M. N., & Ragab M. F., et al., 2022. Coriander (*Coriandrum sativum* L.) essential oil and oil-loaded nano-formulations as an anti-aging potentiality via TGFβ/SMAD pathway. *Sci. Rep.*; 12:1–15. doi: 10.1038/s41598-021-99269-x.

[24] Bentarhlia, N., Kartah, B. E., Fadil, M., El Harkaoui, S., Matthäus, B., Abboussi, O., & El Monfalouti, H.,2024. Exploring the woundhealing and antimicrobial potential of Dittrichia viscosa L lipidic extract: Chemical composition and in vivo evaluation. *Fitoterapia*, 172, 105707.

[25] Harborne J.B. 1973. Phytochemical Methods; A guide to modern techniques of plant Analysis.2nd Edition, London New York.

[26] Singleton, V. L. & Rossi, J. A., 1965. Colorimetry of total phenolics with phosphomolybdicphosphotungstic acid reagents. *Am. J. Enol. Vitic.* 16, 144–158.

[27] Tempel, A. S., 1982. Tannin-measuring techniques: A review. *J. Chem. Ecol*. 8(10), 1289–1298.

[28] Hostettmann, K. & Hostettmann, M., 1982.Isolation Techniques for Flavonoids in *The Flavonoids: Advances in Research*. (ed. Harborne, J. B. & Mabry, T. J.) 1–18.

[29] Adams, R. P., 1995. Identification of essential oil components by gas chromatography/mass spectroscopy (Allured Publ. Corp.,).

[30] Blois, M., 1958. Antioxidant Determinations by the Use of a Stable Free Radical. *Nature* 181, 1199–1200.

[31] Re, R., Pellegrini, N., Proteggente, A., Pannala, A., Yang, M., & Rice-Evans, C., *et al.,* 1999. Antioxidant activity applying an improved ABTS radical cation decolorization assay. *Free Radic. Biol. Med.* 26(9-10), 1231-1237.

[32] Ruch, R. J., Cheng, S. J. & Klaunig, J. E., 1989. Prevention of cytotoxicity and inhibition of intercellular communication by antioxidant catechins isolated from Chinese green tea. *Carcinogenesis* 10(6), 1003–1008.

[33] Dinis, T. C., Maderia, V. M. & Almeida, L. M., 1994.Action of phenolic derivatives (acetaminophen, salicylate, and 5aminosalicylate) as inhibitors of membrane lipid peroxidation and as peroxyl radical scavengers. *Arch. Biochem. Biophys*. 315(1), 161–169.

[34] Wagdi, M. A., Salama, A., El-Liethy, M. A. & Shalaby, E. S., 2023. Comparative study of niosomes and spanlastics as a promising approach for enhancing benzalkonium chloride topical wound healing: *In-vitro* and *in-vivo* studies. *J. Drug Deliv. Sci. Tec.* 84, 1044-1056.

[35] Kamal, N.H., Saber, F.R., Salama, A. El-Hefnawy, H. M. & Meselhy, M. R., 2024. Enhanced wound healing activity of naturally derived Lagenaria siceraria seed oil binary nanoethosomal gel: formulation, characterization, in vitro/in vivo efficiency. Futur J Pharm. Sci. 10, 102. https://doi.org/10.1186/s43094-024-00678-2.

[36] Anwar, M. A., El Gedaily, R. A., Salama, A., Aboulthana, W. M., Kandil, Z. A. & Abdeldayem, S. I.A., 2025. Phytochemical analysis and wound healing properties of *Malva parviflora* L. ethanolic extract. Journal of Ethnopharmacology, 337(3), 118983. https://doi.org/10.1016/j.jep.2024.118983.

[37] Asfour, M. H., Elmotasem, H., Mostafa, D. M. & Salama, A. A. A., 2017 Chitosan based Pickering emulsion as a promising approach for topical application of rutin in a solubilized form intended for wound healing: *In vitro* and *in vivo* study. *Int. J. Pharm.* 534(1-2), 325–338.

[38] Salama, A., Moustafa, P.E. & Elgohary, R., 2024. Exploring Echinacea purpurea's effect on wound healing in rats: FOXO1/MIP2 pathway modulation. Comp. Clin. Pathol. 33, 277–286. https://doi.org/10.1007/s00580-023-03549-z.

[39] Bancroft, J. D. & Layton, C. 2013. The hematoxylins and eosin in *Bancroft's Theory and Practice of Histological Techniques* (ed. Suvarnam, S. K., Layton, C. & Bancroft, J. D.) 173-186 (Churchill Livingstone,).

[40] Agu, P. C., Afiukwa, C. A., Orji, O. U., Ezeh, E. M., & Ofoke, I. H., *et al.,* 2023. Molecular docking as a tool for the discovery of molecular targets of nutraceuticals in diseases management. *Sci. Rep.* 13(1), 13398. doi: 10.1038/s41598-02340160-2.

[41] Nielsen, A. B. & Holder, A. J. Gauss View 5.0, User's Reference, GAUSSIAN Inc., Pittsburgh (2009).

[42] Becke, A. D., 1993. Density-functional thermochemistry. III. The role of exact exchange. *J. Chem. Phys.* 98, 5648–5652.

[43] Lee, C., Yang, W. & Parr, R. G., 1988. Development of the Colle-Salvetti correlationenergy formula into a functional of the electron density. *Phys. Rev. B Condens. Matter.* 37(2), 785–789.

[44] Miehlich, B., Savin, A., Stoll, H. & Preuss, H. 1989. Results obtained with the correlation energy density functionals of becke and Lee, Yang and Parr. *Chem. Phys. Lett.* 157(3), 200– 206.

[45] Langendorf, C., Ngoei, K. R. W., Scott, J. W. L., Naomi, X. Y., & Sam M. A., *et al.,* 2016. Structural basis of allosteric and synergistic activation of AMPK by furan-2-phosphonic derivative C2 binding. *Nat. Commun.* 7, 109-112.

[46] Lovejoy, B. Cleasby, A. Hassell, A. M., Longley, K., & Luther, M. A., *et al.,* 1994. Structure of the catalytic domain of fibroblast collagenase complexed with an inhibitor. *Science* 263(5145), 375–377.

[47] Moon, H., Han, S., Park, H. & Choe, J. 2010. Crystal structures of human FIH-1 in complex with quinol family inhibitors. *Mol. Cells* 29(5), 471–474.

[48] Rowsell, S. Hawtin, P., Minshull, C. A., Jepson, H., & Brockbank, S. M. V., *et al.,* 2002. Crystal structure of human MMP9 in complex with a reverse hydroxamate inhibitor. *J. Mol. Biol.* 319(1), 173–181.

[49] He, M. M., Smith, A. S., Oslob, J. D. M., Flanagan, W., & Braisted, A. C., *et al.,* 2005.

Small-molecule inhibition of TNF-alpha. *Science* 310(5750), 1022–1025.

[50] Wiesmann, C., Fuh, G., Christinger, H., W., Eigenbrot, C., & Wells, J. A., *et al.,* 1997. Crystal structure at 1.7 A resolution of VEGF in complex with domain 2 of the Flt-1 receptor. *Cell* 91(5), 695–704.

[51] Kaplan, W. & Littlejohn, T. G., 2001. Swiss-PDB Viewer (Deep View). *Brief Bioinform.* 2(2), 195– 197.

[52] Morris, G. M., Huey, R., Lindstrom, W., Sanner, M. F., & Belew, R. K., *et al.*, 2009. AutoDock4 and AutoDockTools4: Automated docking with selective receptor flexibility. *J. Comput. Chem.* 30(16), 2785–2791.

[53] Wilkinson, H. N. & Hardman, M. J., 2020. Wound healing: Cellular mechanisms and pathological outcomes. *Open Biol*. 10(9), 20022023.

[54] Nussbaum, S. R., Carter, M. J., Fife, C. E., DaVanzo, J., & Haught, R., *et al.,* 2018. An Economic Evaluation of the Impact, Cost, and Medicare Policy Implications of Chronic Nonhealing Wounds. *Value Health* 21(1), 27–32.

[55] Elbialy, Z. I. Atiba, A., Abdelnaby, A., AlHawary, I. I., & Elsheshtawy, A., *et al.,* 2020. Collagen extract obtained from Nile tilapia (*Oreochromis niloticus* L.) skin accelerates wound healing in rat model via up regulating VEGF, bFGF, and α-SMA genes expression. *BMC Vet. Res.* 16, 352. doi: 10.1186/s12917-02002566-2.

[56] Kamel, R., El-Batanony, R. & Salama, A., 2019. Pioglitazone-loaded three-dimensional composite polymeric scaffolds: A proof of concept study in wounded diabetic rats. *Int. J. Pharm.* 570, 118667).

[57] Huang, H., Wang, L., Qian, F., Chen, X., & Zhu, H., *et al.,* 2021. Liraglutide *via* activation of AMP-activated protein kinase-hypoxia inducible factor-1α-heme oxygenase-1 signaling promotes wound healing by preventing endothelial dysfunction in diabetic mice. *Front. Physiol.* 12, 660263. doi: 10.3389/fphys.2021.660263.

[58] Hong, W. X., Hu, M. S., Esquivel, M., Liang, G. Y., & Rennert, R. C., *et al.* ,2014. The Role of Hypoxia-Inducible Factor in Wound Healing. *Adv. Wound Care (New Rochelle)* 3(5), 390–399.

[59] Giostri, G. S. Novak, E., M., Buzzi, M., Guarita& Souza, L. C. 2022. Treatment of acute wounds in hand with *Calendula officinalis* L.: A randomized trial. *Tissue Barriers* 10(3), 1994822. doi: 10.1080/21688370.2021.

[60] Fronza, M., Heinzmann, B., Hamburger, M., Laufer, S., & Merfort, I., 2009. Determination of the wound healing effect of *Calendula* extracts using the scratch assay with 3T3 fibroblasts. *J. Ethnopharmacol.* 126(3), 463–467.

[61] Zaki, M. M., Abo Elhassan, A. E., El Zahid, E. S. M., Ahmed, M. K. A., Hejab, A. M. I., Kamel, A. H., Amin, T. R. & Hassan, S. S. M., 2023. Phytochemical screening and toxicity studies for ginger extracts with evaluation of some biochemical parameters and anticoagulant bioactivity. *Egypt. J. Chem.* 66(13), 2389–2406.

[62] Sapkota, B. & Kunwar, P., 2024. A Review on Traditional Uses, Phytochemistry and Pharmacological Activities of *Calendula officinalis* Linn. *Natural Product Communications*, 19(6), doi.org/10.1177/1934578X241259021.

[63] Verma, N., & Shukla, S., 2015. Impact of various factors responsible for fluctuation in plant secondary metabolites. *Journal of Applied Research on Medicinal and Aromatic Plants,* 2(4), 105–113.

[64] Scarano, A., Laddomada, B., Blando, F., De Santis, S., Verna, G., Chieppa, M., & Santino, A. 2023. The chelating ability of plant polyphenols can affect iron homeostasis and gut microbiota. *Antioxidants*, *12*(3), 630.

[65] Hassanpour, S. H., & Doroudi, A., 2023. Review of the antioxidant potential of flavonoids as a subgroup of polyphenols and partial substitute for synthetic antioxidants. *Avicenna journal of phytomedicine*, *13* (4), 354.

[66] Rigane, G., Ben Younes, S., Ghazghazi, H., & Ben Salem, R., 2013. Investigation into the biological activities and chemical composition of Calendula officinalis L. growing in Tunisia., *International Food Research Journal*, 20(6), 3001–3007

[67] Naczk, M., & Shahidi, F., 2006. Phenolics in cereals, fruits and vegetables: Occurrence, extraction and analysis. *Journal of pharmaceutical and biomedical analysis*., 41(5), 1523–1542.

[68] Massoud, H. Y., El-Kafie, A., Omaima, M., Helaly, A.A., & Ghanem, M.E. 2020. Genetic variability studies in *Calendula officinalis* plant. *Journal of Plant Production*, *11*(5), 425– 428.

[69] Ak, G., Zengin, G., Sinan, K. I., Mahomoodally, M. F., Picot-Allain, M. C. N., Cakır, O., & Montesano, D., 2020. A comparative bioevaluation and chemical profiles of *Calendula officinalis L*. extracts

prepared via different extraction techniques. *Applied sciences,* 10(17), 5920.

[70] Venkatesh, D. P., Gheena, S., Ramani, P., Rajeshkumar, S., & Ramalingam, K., 2023.In Vitro Evaluation of Antioxidant and Antiinflammatory Potentials of Herbal Formulation Containing Marigold Flower (*Calendula officinalis L.*) Tea. *Cureus*,15(8).

[71] Sahingil, D., 2019. GC/MS-olfactometric characterization of the volatile compounds, determination antimicrobial and antioxidant activity of essential oil from flowers of calendula (*Calendula officinalis* L.). *J. Essent. Oil Bear. Pl.* 22(6), 1571–1580.

[72] Hadi, M. Y., Mohammed, G. J. & Hameed, I. H., 2016. Analysis of bioactive chemical compounds of *Nigella sativa* using gas chromatography-mass spectrometry. *J. Pharmacogn. Phytotherapy* 8(2), 8–24.

[73] McDaniel, J. C., Belury, M., Ahijevych, K. & Blakely. W. 2008. Omega-3 fatty acids effect on wound healing. *Wound Repair Regen.* 16(3), 337–345.

[74] Balić, A., Vlašić, D., Žužul, K., Marinović, B. & Bukvić Mokos, Z., 2020. Omega-3 versus omega6 polyunsaturated fatty acids in the prevention and treatment of inflammatory skin diseases. *Int. J. Mol. Sci.* 21(3), 741.

[75] Škapars, R. Gašenko, E., Broza, Y. Y., Sīviņš, A., & Poļaka, I., *et al.,* 2023. Breath Volatile Organic Compounds in Surveillance of Gastric Cancer Patients following Radical Surgical Management. *Diagnostics* 13(10), 1670. doi: 10.3390/diagnostics13101670.

[76] Shoaib, M., Shah, I., Ali, N., Adhikari, A., & Tahir M. N., *et al.,* 2017. Sesquiterpene lactone! a promising antioxidant, anticancer and moderate antinociceptive agent from *Artemisia macrocephala* jacquem. *BMC Complement. Altern. Med.* 17, 27. doi: 10.1186/s12906-0161517-y.

[77] Osuntokun, O. T., Oluduro, A. O., Idowu, T. O. & Omotuyi, A. O., 2017. Assessment of Nephrotoxicity, Anti-Inflammatory and Antioxidant Properties of Epigallocatechin, Epicatechin and Stigmasterol Phytosterol (Synergy) Derived from Ethyl Acetate Stem Bark Extract of *Spondias Mombin* on Wistar Rats Using Molecular Method of Analysis. *J. Mol. Microbiol.* 1(1), 5.

[78] Ashraf, R. & Bhatti, H.N., 2021.Stigmasterol in *A Centum of Valuable Plant Bioactives* (eds. Mushtaq, M. & Anwar, F.) 213–232.

[79] la Torre Fabiola, V. D., Ralf, K., Gabriel, B., Ermilo, A. V., & Martha M., *et al.,* 2016. Antiinflammatory and immunomodulatory effects of *Critonia aromatisans* leaves: Downregulation of pro-inflammatory cytokines. *J. Ethnopharmacol*. 190, 174–182.

[80] Mohamed, N. T., Abdelsalam, D. H., El-Ebiarie, A. S. & Elaasser, M., 2021. Seperation of bioactive compounds from Haemolymph of scarab beetle *Scarabaeus sacer* (Coleoptera: Scarabaeidae) by GC-MS and determination of its antimicrobial activity. *International Journal of Applied Biology and Pharmaceutical Technology* 12, 461–480.

[81] Shi, X. Q. Chen, G., Tan, J., Li, Z., & Chen, S., *et al.,* 2022. Total alkaloid fraction of *Leonurus japonicus* Houtt. Promotes angiogenesis and wound healing through SRC/MEK/ERK signaling pathway. *J. Ethnopharmacol.* 295, 115396. doi.org/10.1016/j.jep.2022.115396

[82] Balachandran, A., Choi, S. B., Beata, M., Małgorzata, J., & Froemming, G. R. A., *et al.,* 2023. Antioxidant, Wound Healing Potential and In Silico Assessment of Naringin, Eicosane and Octacosane. *Molecules* 28(3), 1043. doi: 10.3390/molecules28031043.

[83] Al-Rajhi, A. M. H. Qanash , H., Almuhayawi, M. S., Al Jaouni, S., K., & Bakri M. M., *et al.,* 2022. Molecular Interaction Studies and Phytochemical Characterization of *Mentha pulegium* L. Constituents with Multiple Biological Utilities as Antioxidant, Antimicrobial, Anticancer and AntiHemolytic Agents. *Molecules* 27(15), 4824. doi: 10.3390/molecules27154824.

[84] Preethi, K. C., Siveen, K. S., Kuttan, R. & Kuttan, G., 2010.Inhibition of Metastasis of B16F-10 Melanoma Cells in C57BL/6 Mice by an Extract of *Calendula Officinalis* L. Flowers. *Asian Pac. J. Cancer Prev*. **11**(6), 1773–1779.

[85] Chen, D. Qanash , H., Almuhayawi, M. S., Al Jaouni, S., K., & Bakri M. M., *et al.,* 2016. Regulation of protein-ligand binding affinity by hydrogen bond pairing. *Sci. Adv*. 2(3), e1501240. doi: 10.3390/molecules27154824.

[86] Schiebel, J. Gaspari, R., Wulsdorf, T., Ngo, K., & Sohn C., *et al.,* 2018 Intriguing role of water in protein-ligand binding studied by neutron crystallography on trypsin complexes. *Nat. Commun.* 9, 3559. doi: 10.1038/s4146